A semiphenomenological droplet model of homogeneous nucleation from the vapor phase

Can F. Delale, and Gerd E. A. Meier

AIP | The Journal of Chemical Physics

PERSPECTIVES
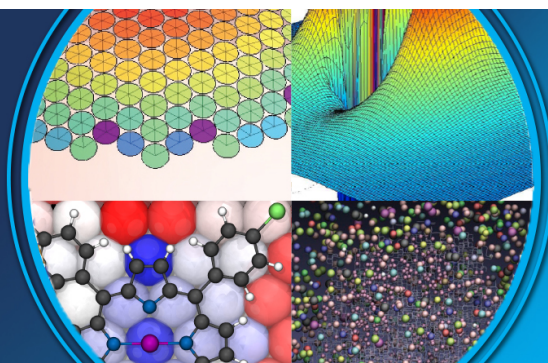
A semiphenomenological droplet model of homogeneous nucleation from the vapor phase

Can F. Delale[a)]
Max Planck Institut für Strömungsforschung, Bunsenstrasse 10, D 3400 Göttingen, Germany, and Department of Mathematics, Bilkent University, 06533 Bilkent, Ankara, Turkey

Gerd E. A. Meier
DLR Institut für Experimentelle Strömungsmechanik, Bunsenstrasse 10, D 3400 Göttingen, Germany

A semiphenomenological droplet model, which corrects for the macroscopic surface tension and monomer–monomer interactions from real gas behavior (second virial coefficient) and for the correlation between the mean surface area of a cluster and the number of molecules constituting the cluster over all ranges of temperature below the critical point, is proposed by modifying Fisher's droplet theory of condensation. A steady-state nucleation rate equation is derived and compared with expansion and diffusion cloud chamber data for a variety of substances. An overall good agreement is achieved for the range of temperatures investigated in contrast to comparison with the classical nucleation rate equation.

I. INTRODUCTION

The kinetics of phase transitions has rather a broad field of applications in science and technology from astrophysics to biology. In particular, the kinetics of condensation from the vapor phase, which is the subject of this investigation, is described by the generation of condensation nuclei that grow into droplets in the metastable vapor state. Such nuclei may either form in the interior of the parent phase (homogeneous nucleation) or on ions, impurity molecules, dust particles, etc. present in the parent phase (heterogeneous nucleation). Only homogeneous nucleation theory is considered in this study.

The theory of homogeneous nucleation has already been discussed for many years in various studies.[1–3] It was originated by Volmer and Weber[4] using Gibbs' capillarity approximation and further refined by Farkas,[5] Becker and Döring,[6] Volmer,[1] Zel'dovich,[7] and Frenkel[8] in developing into what today is commonly referred to as the classical nucleation theory. However, with the advent of experimental techniques in the last decades,[9–18] it has been reported that classical theory yields nucleation rates which are sometimes off by several orders of magnitude in comparison with experiments. The attempts by Lothe and Pound,[19] Reiss, Katz, and Cohen,[20] Courtney,[21] and Feder et al.[22] to improve the theory by taking into account the various degrees of freedoms (translational, rotational, vibrational, configurational, etc.) and the nonequilibrium effects left out in the classical theory have to some extent improved our understanding of the phenomenon, however, they have not proved successful in comparison with experiments (predicted nucleation rates by some of these theories are sometimes off by a factor of 10^{17}). A consistent theory of homogeneous nucleation which agrees well with the measured nucleation rates is still in need.

Recently, Dillmann and Meier[23] have proposed a semiphenomenological model based on Fisher's cluster theory of condensation and metastability.[24] They achieve good agreement with reliable experimental data for a variety of substances by their proposed nucleation rate equation. However, the model contains inconsistencies arising from employing the ideal gas equation for monomers (clusters containing only one molecule) on the one hand and the virial equation of state of a real gas for the vapor phase on the other hand (e.g., see Ford[25]) as well as from approximating the mean surface area of a cluster by its geometric value. The aim of the present investigation is to overcome these inconsistencies without spoiling the agreement with the experiments. For this reason, a consistent semiphenomenological droplet model based on the actual virial equation of state is constructed by slightly modifying Fisher's cluster theory, and a steady-state nucleation rate equation that follows from this model is derived. Good agreement with the experimental nucleation rates is achieved for all substances over the range of temperatures investigated.

II. EQUILIBRIUM CLUSTER DISTRIBUTION IN THE METASTABLE VAPOR STATE

We consider an extension of Fisher's droplet or cluster theory[24] of condensation and assume that a cluster A_i containing i molecules (i mer) can only grow or shrink by monomolecular association or dissociation

$$A_i + A_1 \rightleftharpoons A_{i+1} \quad (i=1,2,...). \tag{1}$$
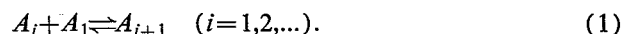
Following Band,[26] the equilibrium number distribution N_i of i mers for reaction (1) can be evaluated by

$$N_i = Z_i \exp\left(\frac{i\mu_v}{kT}\right), \tag{2}$$

where $Z_i \equiv \exp(-F_i/kT)$ is the partition function of an i mer with F_i denoting its Helmholtz free energy, k is Boltzmann's constant, μ_v is the chemical potential of monomers, and T is the temperature. In arriving at Eq. (2), it is implicit that the interactions between clusters of size $i \geqslant 2$ and the monomers are neglected; therefore, real gas effects

of the vapor phase can only arise from monomer–monomer interactions. If we also consider the equality $f_\infty = \mu_{v,\mathrm{coex}}$, where $\mu_{v,\mathrm{coex}}$ is the chemical potential and f_∞ is the Helmholtz free energy per molecule of the bulk liquid phase on the vapor–liquid coexistence line, from Eq. (2) we arrive at the fundamental expression for the equilibrium number density n_i of i mers as

$$n_i = \frac{N_i}{V} = \frac{1}{V} \exp\left(-\frac{\Delta G_i}{kT}\right) \tag{3}$$

with

$$\Delta G_i \equiv (F_i - if_\infty) - i(\mu_v - \mu_{v,\mathrm{coex}}) \equiv \Delta F_i - i\Delta\mu, \tag{4}$$

where ΔG_i the Gibbs free energy of formation is the reversible work necessary to form an i mer from i molecules of the bulk liquid phase and V is the volume. The number density n of the vapor can then be related to the i-mer number density n_i by

$$n = \sum_{i=1}^{\infty} i n_i. \tag{5}$$

If in addition monomers (thereby the vapor) are treated as an ideal gas, the pressure of the mixture can be evaluated by Dalton's law as

$$p = kT \sum_{i=1}^{\infty} n_i. \tag{6}$$

Equations (3)–(6) are the equations commonly employed in nucleation theory and neglect any possible cluster–cluster interactions. However, if clustering is thought to result from real gas behavior of the vapor, at least monomer–monomer interactions cannot be neglected since most of the clusters present in the vapor are in the form of monomers. This implies that one should really abandon Eq. (6) (otherwise inconsistencies arise) and instead employ the virial equation of state in the form

$$\frac{p}{n} = kT + \sum_{j=2}^{\infty} B_j p^{(j-1)} = kT + B_2 p + B_3 p^2 + \cdots, \tag{7}$$

where B_j, $j = 2,3,...$ are the temperature dependent virial coefficients presumably to be given for a chosen vapor. Equations (3), (4), (5), and (7) are the basic equations of the proposed semiphenomenological droplet model. What remains to be determined is the form of the Gibbs energy of formation, or equivalently the estimation of $\Delta\mu$ and ΔF_i in Eq. (4). The chemical potential μ_v of monomers is given by the well-known formula[27]

$$\mu_v(T,p_1,N_1) = [\mu_v(T,p_1)]_{\mathrm{ideal}} + \int_0^{p_1} \left(\frac{\partial V}{\partial N_1} - \frac{kT}{p'}\right) dp', \tag{8}$$

where

$$[\mu_v(T,p)]_{\mathrm{ideal}} = \mu_v^0(T) + kT \ln p \tag{9}$$

with $\mu_v^0(T)$ being the chemical potential as $p \to 0$. As mentioned earlier, since the number of monomers in the vapor are expected to be much greater than the total number of molecules bound in higher clusters, the number density n_1

of monomers and consequently their partial pressure p_1 can to a good approximation be taken as the total number density n and the total pressure p, respectively, in evaluating Eq. (8). With this in mind, substitution from Eq. (7) into Eq. (8) yields

$$\Delta\mu \equiv \mu_v - \mu_{v,\mathrm{coex}}$$
$$\approx kT \ln S + \sum_{j=2}^{\infty} \frac{B_j p_{\mathrm{sat}}^{(j-1)}}{(j-1)} (S^{(j-1)} - 1)$$
$$= kT \ln S + B_2 p_{\mathrm{sat}}(S-1) + \frac{B_3 p_{\mathrm{sat}}^2}{2}(S^2 - 1) + \cdots, \tag{10}$$

where

$$S \equiv \frac{p}{p_{\mathrm{sat}}} \tag{11}$$

is the supersaturation and p_{sat} is the saturation pressure at T. Having estimated $\Delta\mu$ in Eq. (4), we suggest a generalized phenomenological form for the difference ΔF_i of Helmholtz free energies F_i and if_∞ as (it is well known that ΔF_i cannot totally be determined from thermodynamics or statistical mechanics)

$$\Delta F_i = \lambda_i \gamma s_1 i^{\sigma_i} + \tau kT \ln i - kT \ln(q_0 V) \tag{12}$$

for $i = 1,2,...$, where q_0 and τ are parameters to be determined, γ is the macroscopic surface tension, and λ_i are functions of size and temperature which describe deviations of the surface energy from that of a macroscopic liquid droplet satisfying the limiting condition (e.g., see Sinanoğlu[28])

$$\lambda_\infty \equiv \lim_{i \to \infty} \lambda_i = 1. \tag{13}$$

The term $s_1 i^{\sigma_i}$ of Eq. (12) is the mean surface area of an i mer, where the unknown functions σ_i, in general size and temperature dependent, characterize the correlation between the mean surface area and the number of molecules of an i mer with the limiting condition

$$\sigma_\infty \equiv \lim_{i \to \infty} \sigma_i = \frac{2}{3} \tag{14}$$

corresponding to its geometrical value, and where s_1 given by

$$s_1 = \left(6\sqrt{\pi} \frac{m_1}{\rho_l}\right)^{2/3} \tag{15}$$

is the mean surface area of a single molecule in the bulk liquid phase with m_1 and ρ_l denoting, respectively, the mass of a single molecule and the density of the bulk liquid phase. In particular, the second and third terms of Eq. (12) signify the contributions to the free energy arising from the translational, rotational, vibrational, and configurational degrees of freedom[23,29] and all droplet models can be regarded as special cases of Eq. (12) depending on the values of the parameters τ and q_0, provided that in all cases $\sigma_i = 2/3$ and λ_i is set equal to unity for all i. For example, the classical theory is obtained with $\tau = 0$, the

Lothe–Pound theory results when $\tau = -4$, and the Reiss–Katz–Cohen theory is approached with $-3/2 < \tau < -1/2$. Each theory yields its own value for q_0.

We now discuss how we can determine the functions σ_i and λ_i. It has already been mentioned that σ_∞ assumes the geometric value 2/3. In general, at any fixed temperature, σ_i oscillates with respect to the number of molecules i in a cluster. This means that addition of a single molecule to the i mer or cluster may change the correlation between the mean surface area of the cluster and the number of molecules contained due to the many body interaction potentials of the new configuration unless the cluster contains sufficiently large number of molecules so that σ assumes its geometric value 2/3. In any finite interval of i, σ_i will fluctuate about a mean value, and if the interval is chosen small enough, fluctuations in σ_i can be neglected with respect to the mean value over the interval. From stability considerations, the interval of interest for condensation theory is $1 \leqslant i \leqslant i^*$, where i^* is the critical number of molecules in a cluster beyond which the cluster acts as a condensation nucleus and grows into a droplet (i^* corresponds to a maximum of the Gibbs formation energy ΔG_i with respect to i). Thus neglecting fluctuations, we can assume that σ_i may as well be approximated by its temperature dependent mean value $\sigma = \sigma(T)$ over this interval. Actually this assumption was taken for granted for all i in Fisher's droplet model[24] where σ was shown to satisfy

$$0 < \sigma < 1. \tag{16}$$

We will leave out the discussion of the temperature dependence of σ to the next sections and proceed to determine the functions λ_i. For this reason, we first evaluate the number density n utilizing Eqs. (3)–(5), (10), and (12) to arrive at

$$n = q_0 \sum_{i=1}^{\infty} S^i i^{-(\tau-1)} \exp\left[-\lambda_i \theta i^\sigma \right.$$
$$\left. + \frac{i}{kT} \sum_{j=2}^{\infty} \frac{B_j p_{\text{sat}}^{(j-1)}}{(j-1)} (S^{(j-1)} - 1) \right], \tag{17}$$

which evaluates to

$$n = q_0 \sum_{i=1}^{\infty} [\chi(T)]^i S^i i^{-(\tau-1)} \exp(-\lambda_i \theta i^\sigma) \left[1 + \frac{B_2 p_{\text{sat}}}{kT} S \right.$$
$$\left. + \frac{1}{2} \left(\frac{p_{\text{sat}}}{kT} \right)^2 (B_2^2 + kT B_3) S^2 + \cdots \right]^i, \tag{18}$$

where

$$\chi(T) \equiv \exp\left[-\frac{1}{kT} \sum_{j=2}^{\infty} \frac{B_j p_{\text{sat}}^{(j-1)}}{(j-1)} \right]$$
$$= \exp\left(-\frac{B_2 p_{\text{sat}}}{kT} - \frac{B_3 p_{\text{sat}}^2}{2kT} - \cdots \right) \tag{19}$$

and

$$\theta \equiv \frac{\gamma s_1}{kT}. \tag{20}$$

Now substitution from Eq. (18) to the virial equation of state (7) and collecting together equal powers of p determine the functions λ_i,

$$\lambda_1 = -\frac{1}{\theta} \ln\left[\frac{p_{\text{sat}}}{q_0 kT \chi(T)} \right], \tag{21}$$

$$\lambda_2 = -\frac{1}{\theta 2^\sigma} \ln\left\{ \left[\frac{p_{\text{sat}}}{q_0 kT \chi(T)} \right]^2 (-B_2 q_0) 2^\tau \right\}, \tag{22}$$

$$\lambda_3 = -\frac{1}{\theta 3^\sigma} \ln\left\{ \frac{1}{2} \left[\frac{p_{\text{sat}}}{q_0 kT \chi(T)} \right]^3 (3B_2^2 - kT B_3) q_0^2 3^\tau \right\}, \tag{23}$$

etc. It should be noticed that the functions λ_1 and λ_2 differ from the functions κ_1 and κ_2 of Dillmann and Meier[23] by an additional factor $\chi(T)$ and by replacement of τ in Eq. (22) by $(\tau - 1)$ as mentioned by Ford[25] as well. It is now clear from Eqs. (21)–(23) that the evaluation of λ_i requires a knowledge of the ith virial coefficient B_i. In general, knowledge of the virial coefficients beyond B_2 is either poorly known or not available. Thus we would like to determine λ_i from a knowledge of the second virial coefficient B_2 alone in terms of λ_1 and λ_2. This is possible since the work of different authors[30,31] indicates that λ_i is of the form

$$\lambda_i = f\left(\frac{a}{r_i} \right), \tag{24}$$

where $r_i \sim i^{\sigma_i/2}$ is the mean spherical radius of an i mer and a is some characteristic submolecular length much smaller than the radius of a monomer ($a \ll r_1$). Thus by expanding f in a Taylor series under the limiting condition (13), the functions λ_i can be approximated by[23,31]

$$\lambda_i = 1 + \alpha_1 i^{-\sigma_i/2} + \alpha_2 i^{-\sigma_i} \tag{25}$$

for all i. In particular, in the interval $1 \leqslant i \leqslant i^*$, we have from the above consideration $\sigma_i = \sigma$. The parameters α_1 and α_2 then follow from Eq. (25) as

$$\alpha_1 = \frac{2^\sigma(\lambda_2 - 1) - (\lambda_1 - 1)}{2^{\sigma/2} - 1} \tag{26}$$

and

$$\alpha_2 = \frac{2^{\sigma/2}(\lambda_1 - 1) - 2^\sigma(\lambda_2 - 1)}{2^{\sigma/2} - 1}, \tag{27}$$

where λ_1 and λ_2 are given by Eqs. (21) and (22). The equilibrium cluster distribution of an i mer can now be obtained from knowledge of the macroscopic surface tension γ, the second virial coefficient B_2, and the density of the saturated liquid ρ_l in the form

$$n_i = q_0 [\chi(T)]^i \exp\left[-\lambda_i \theta i^\sigma - \tau \ln i + i \left(\ln S + \frac{B_2 p_{\text{sat}}}{kT} S \right) \right],$$
$$i = 1, 2, \ldots, i^*, \tag{28}$$

where

$$\chi(T) = \exp\left(-\frac{B_2 p_{\text{sat}}}{kT} \right) \tag{29}$$

TABLE I. Experimental and theoretical values of the critical exponents β and δ (Ref. 33) and of σ_c and τ [Eqs. (30) and (31)].

	β	δ	σ_c	τ
Experimental	0.320–0.330	4.727–4.906	0.611–0.661	2.204–2.212
Renormalization group	0.324–0.327	4.795–4.842	0.633–0.645	2.207–2.208
High temperature series	0.307–0.317	4.918–5.065	0.623–0.662	2.200–2.203

with λ_i given by Eqs. (25)–(27). For a complete description, we still need to know the value of the parameters q_0 and τ and the form of the function $\sigma = \sigma(T)$. This requires a discussion of near critical behavior.

III. BEHAVIOR NEAR THE CRITICAL POINT

The behavior of the droplet model near the critical point was first studied by Fisher[24] leaving out the excluded volume effects (cluster–cluster interactions). He arrived at the relations

$$\sigma_c \equiv \sigma(T_c) = \frac{1}{\beta\delta} \tag{30}$$

and

$$\tau = 2 + \frac{1}{\delta}, \tag{31}$$

where subscript c denotes values at the critical point and where β and δ are three-dimensional universal critical exponents.[24] Since we have presumably taken into account some of the excluded volume effects by employing the phenomenological virial equation of state (7) instead of Eq. (6) used by Fisher and other investigators, the question whether or not relations (30) and (31) remain valid when monomer–monomer interactions are considered naturally arises. This question was partially answered by Stauffer and Kiang[32] who considered the "second virial coefficient" of the hard sphere droplet–droplet interaction. Their conclusion was that relations (30) and (31) still remained valid. This result inspires us to assume that relations (30) and (31) also remain unchanged in our semiphenomenological model where the actual second virial coefficient of the vapor is thought to account for monomer–monomer interactions as well as for the interactions of molecules forming a cluster. Table I (from Beysens[33]) shows the experimental, the renormalization group, and the high temperature series expansion values of the critical exponents β and δ.

and δ and the corresponding values of σ_c and τ. Thus the parameter τ and the value σ_c of σ at the critical temperature can be taken from this table. On the other hand, the parameter q_0 follows directly from Eq. (17) evaluated at $T = T_c$, where $\theta = 0$ and $S = 1$,

$$q_0 = \frac{n_c}{\zeta(\tau - 1)}, \tag{32}$$

where $\zeta(x)$ is the Riemann zeta function of x and n_c is the critical number density. From the critical behavior, we have thus identified the parameters σ_c, τ, and q_0. It remains to find out the temperature dependence of $\sigma = \sigma(T)$. This will be discussed later in Sec. V.

IV. STEADY-STATE NUCLEATION RATE

The kinetics of reaction (1) where the kinetic process rapidly reaches a steady nonequilibrium state is described in detail in various studies.[2,34] The steady-state current or nucleation rate I (number of condensation nuclei formed per unit volume and time) is given by

$$I = \sqrt{-\frac{1}{2\pi kT}\frac{\partial^2 \Delta G_i}{\partial i^2}\bigg|_{i=i^*}} \, c_{i^*} n_{i^*}, \tag{33}$$

where i^*, given by the maximum of Gibbs formation energy

$$\frac{\partial \Delta G_i}{\partial i}\bigg|_{i=i^*} = 0 \tag{34}$$

(apparently $\partial^2/\partial i^2 \Delta G_i|_{i=i^*} < 0$), is the critical number of molecules in a cluster beyond which the cluster acts as a condensation nucleus and grows into a droplet, n_{i^*} is the equilibrium number density of clusters of critical size, and the kinetic factor c_{i^*} is the rate of monomer impact on the surface of a cluster of critical size and is given by

$$c_{i^*} = \frac{p}{\sqrt{2\pi m_1 kT}} s_{i^*} \tag{35}$$

with $s_{i^*} = s_1 i^{*\sigma}$ denoting the mean surface of a critical cluster of i molecules. The maximum condition (34) with ΔG_i evaluated from the proposed droplet model by combining Eqs. (4), (10), (12), and (25)–(27) together with the assumption $\sigma_i = \sigma$ for $1 \leqslant i \leqslant i^*$ yields the equation for i^*,

$$\sigma \theta i^{*\sigma} + \frac{\sigma}{2}\alpha_1 \theta i^{*\sigma/2} + \tau - i^*\left[\ln S + \frac{B_2 p_{\text{sat}}}{kT}(S-1)\right] = 0. \tag{36}$$

Now Eqs. (33), (35), and (28) with i replaced by i^* together with Eqs. (4), (10), (12), and (25)–(27) yield the steady-state nucleation rate of the proposed droplet model as

$$I = \sqrt{\frac{1}{2\pi}\left[\tau i^{*(2\sigma-2)} + \sigma(1-\sigma)\theta i^{*(3\sigma-2)} + \frac{\sigma}{2}\left(1 - \frac{\sigma}{2}\right)\alpha_1 i^{*(5\sigma-4)/2}\right]\frac{p_{\text{sat}} s_1}{\sqrt{2\pi m_1 kT}} q_0 S}$$

$$\times \exp\left\{-\lambda_{i^*}\theta i^{*\sigma} - \tau\ln i^* + i^*\left[\ln S + \frac{B_2 p_{\text{sat}}}{kT}(S-1)\right]\right\}, \tag{37}$$

TABLE II. Empirical values of C for the substances investigated.

Substance	C
Water	0.045
n-nonane	0.038
Methanol	0.048
Ethanol	0.046
n-propanol	0.048
n-butanol	0.048

where the functions λ_{i*} are given by Eqs. (25)–(27) with i replaced by i^*. All of the values of the free parameters appearing in Eq. (37), except for the temperature dependence of σ which will be discussed in the next section, are already available from the discussion in previous sections. It should also be noticed that when the functions and free parameters of the proposed model assume the "artificial" values $\lambda_i=1$ ($\alpha_1=\alpha_2=0$), $\tau=0$, $\sigma=2/3$, and $q_0=p/(kT)$ together with $B_2\to 0^-$ in Eqs. (36) and (37), we recover precisely the steady-state nucleation rate equation of the classical Becker–Döring–Zel'dovich theory, namely,

$$I_{\text{class}} = \frac{1}{3}\sqrt{\frac{\theta}{\pi}}\,\frac{ps_1}{\sqrt{2\pi m_1 kT}}\,\frac{p}{kT}\exp\left(-\frac{4}{27}\theta^3\ln^{-2}S\right). \quad (38)$$

The steady-state nucleation rate equations for the rest of the known droplet models can also be obtained accordingly from Eqs. (36) and (37) by taking $B_2\to 0^-$, assuming the geometric value $\sigma=2/3$ and using the appropriate values of τ, q_0, and λ_i.

V. COMPARISON WITH EXPERIMENTS

For comparison of the nucleation rate equation of the proposed model given by Eqs. (36) and (37) with experiments, we need no more than a discussion of the temperature dependence of σ for $T \ll T_c$. It has already been mentioned in Sec. III that the critical value σ_c can be obtained by Eq. (30) using the three-dimensional universal critical exponents (see also Table I). It is possible for a cluster
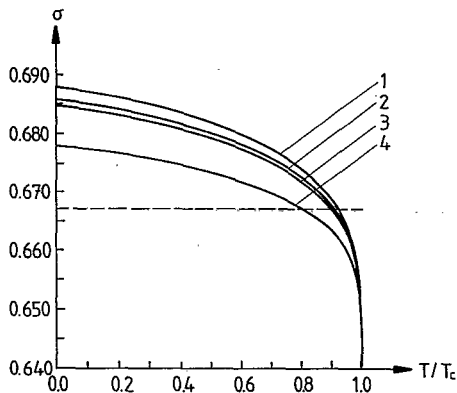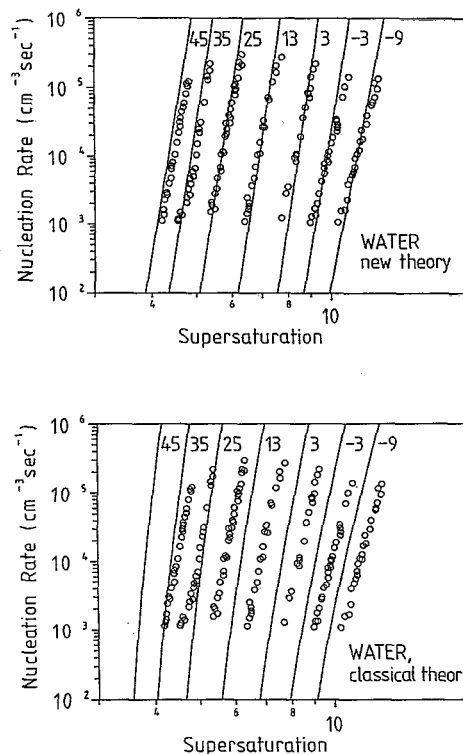

FIG. 2. A comparison of nucleation rates predicted by the classical theory (lower part) and by the new theory (upper part) against expansion cloud chamber data of Miller (open circles) for water (the theoretical solid lines are isentropes, the numbers signify the corresponding initial temperatures in degrees Celsius).
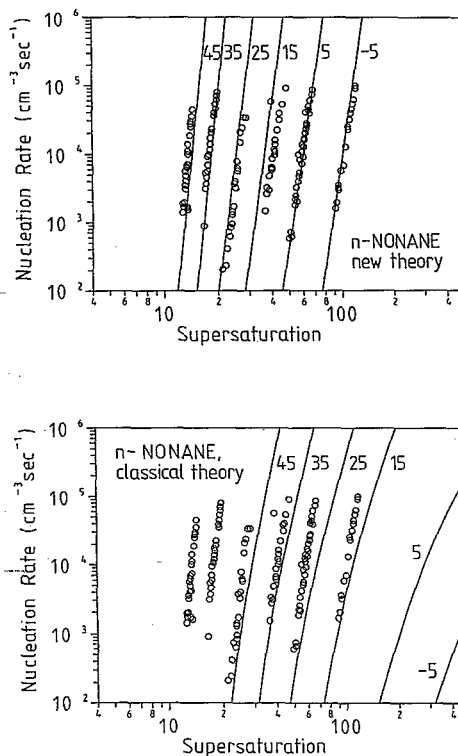

FIG. 1. The variation of σ with temperature [the solid lines are results of Eq. (39) for a variety of substances, namely (1) methanol, n-propanol, n-butanol; (2) ethanol; (3) water; (4) n-nonane, and the dashed line is the geometric value 2/3].

FIG. 3. A comparison of nucleation rates predicted by the classical theory (lower part) and by the new theory (upper part) against expansion cloud chamber data of Adams et al. (open circles) for n-nonane (the theoretical solid lines are isentropes, the numbers signify the corresponding initial temperatures in degrees Celsius).
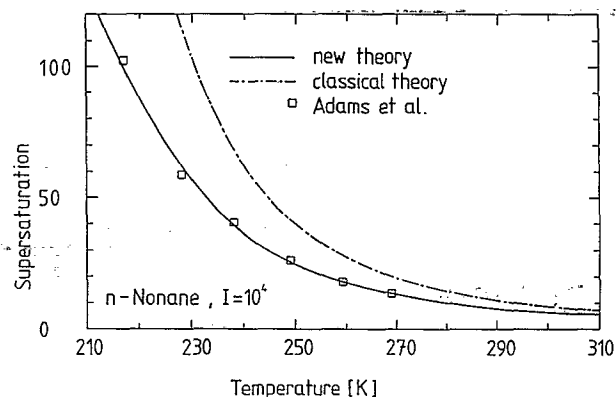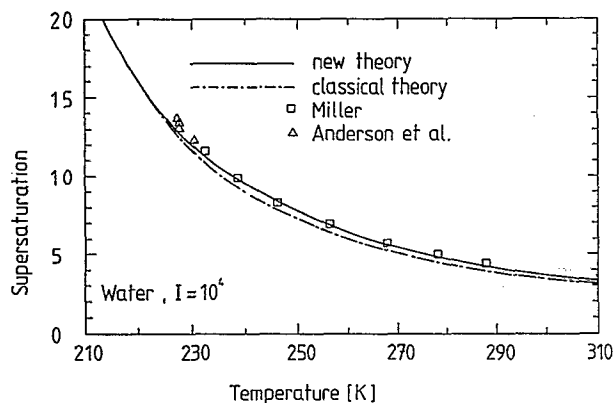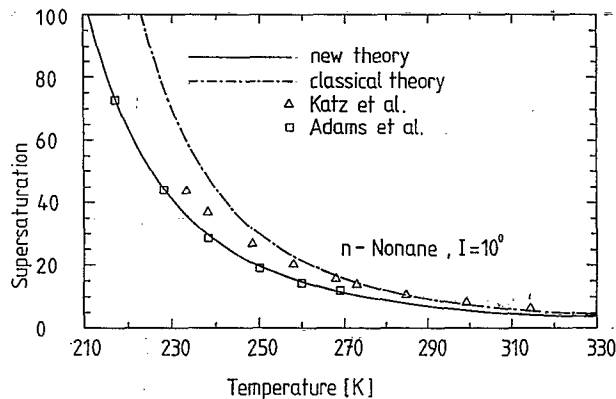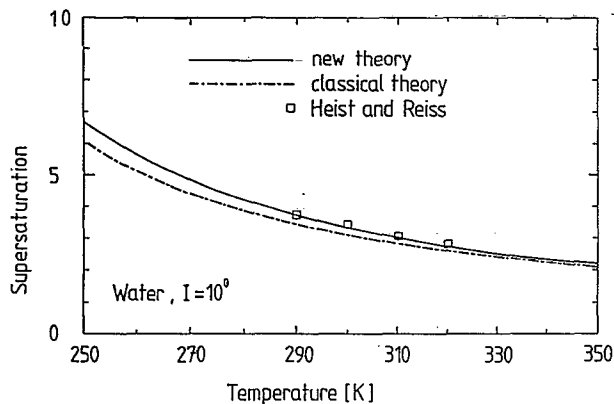
FIG. 4. A comparison of experimental supersaturations with the predictions of the classical theory and the new theory at the constant nucleation rates $I=10^0$ cm^{-3} s^{-1} and $I=10^4$ cm^{-3} s^{-1} for water.

FIG. 5. A comparison of experimental supersaturations with the predictions of the classical theory and the new theory at the constant nucleation rates $I=10^0$ cm^{-3} s^{-1} and $I=10^4$ cm^{-3} s^{-1} for n-nonane.

containing a fixed number of molecules that the mean surface area, thereby σ, is smaller when cluster–cluster interactions are important (apparently closer to the critical point), whereas the more probable larger configurations which occur with a large surface area tend to increase the value of σ (e.g., see Fisher,[24] and Hiley and Sykes[35]). This suggests that σ assumes its minimum value σ_c at the critical point since cluster–cluster interactions are most important there. Thus we can to a good approximation assume a power law for the temperature dependence of σ in the form

$$\sigma=\sigma(T)=\sigma_c+C\left(1-\frac{T}{T_c}\right)^D \tag{39}$$

for $T \leqslant T_c$, where σ_c is given by Eq. (30) and C and D are substance dependent constants. Comparison of nucleation rates by Eqs. (36), (37), and (39) with those of reliable experiments of different substances over a relatively wide range of temperatures suggests that D is the same constant for all substances close to the value 0.2. We herein make the ansatz that D is a universal constant which we take as

$$D=\frac{1}{\delta}, \tag{40}$$

where δ is a universal critical exponent (see Table I). The values of C for the variety of substances investigated are shown in Table II. For these substances, C seems to vary between 0.038 and 0.048. Notice also that the value $C=0.038$ is attained for n-nonane which is the only nonpolar substance investigated, whereas for the other polar substances (water, methanol, etc.), experiments suggest a value of 0.045–0.048 for C. Needless to say that the power law temperature dependence of Eq. (39) for σ together with Eq. (40) for D and the empirical values listed in Table II for C should ultimately be compared with molecular dynamical models, which is outside the scope of this investigation. It is important to mention that the appearance of the constants C (given empirically in Table II) and D [given by Eq. (40)] in Eq. (39) of the proposed model should be regarded as being essential since all previous droplet models suffer quantitatively from the assumption of the mean surface area of a cluster being approximated by its geometric value, i.e., by taking $\sigma=2/3$, which according to Eq. (39) implies the unrealistic values $D=0$ and $C=2/3-\sigma_c$ for all substances and all temperature ranges below T_c. The function $\sigma=\sigma(T)$ is plotted for a variety of substances in Fig. 1. Although experiments show that the deviation of σ from its geometric value 2/3 is small
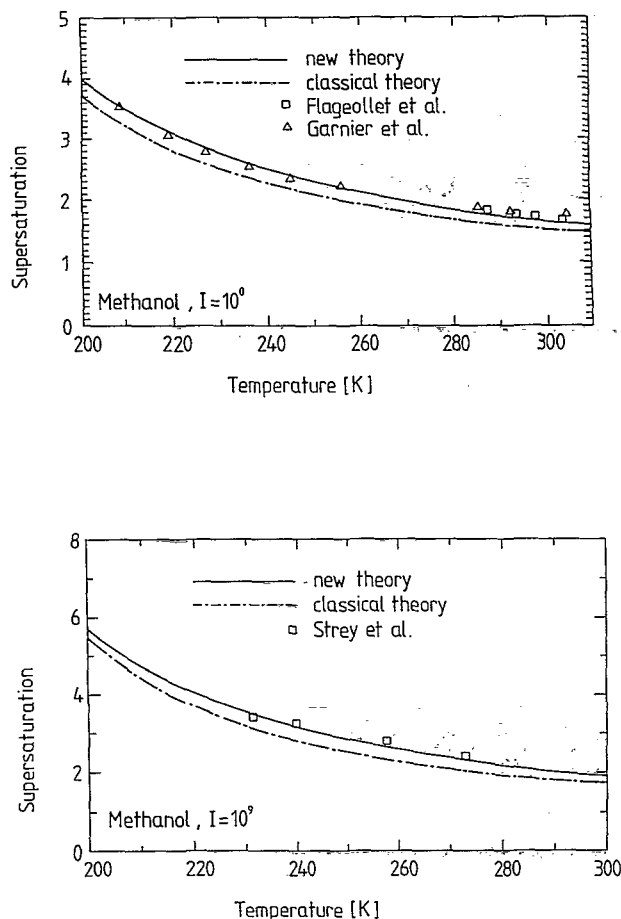
FIG. 6. A comparison of experimental supersaturations with the predictions of the classical theory and the new theory at the constant nucleation rates $I=10^0$ cm^{-3} s^{-1} and $I=10^9$ cm^{-3} s^{-1} for methanol.
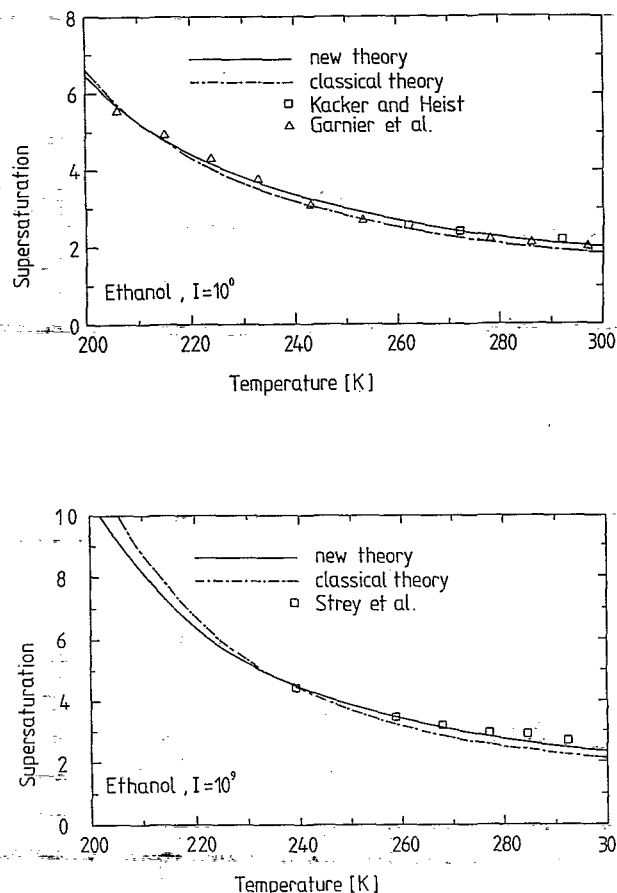
FIG. 7. A comparison of experimental supersaturations with the predictions of the classical theory and the new theory at the constant nucleation rates $I=10^0$ cm^{-3} s^{-1} and $I=10^9$ cm^{-3} s^{-1} for ethanol.

over the range of temperatures investigated, the nucleation rates calculated are effected considerably by orders of magnitude.

We are now in a position to present an algorithm for the calculation of nucleation rates by the proposed model using only macroscopic quantities. The required quantities are

(1) molar mass M or equivalently mass of a single molecule m_1;

(2) critical properties of state (p_c, n_c, and T_c);

(3) the macroscopic surface tension $\gamma(T)$;

(4) the density of the saturated liquid $\rho_l(T)$; and

(5) the second virial coefficient $B_2(T)$. These quantities for a variety of substances over a relatively broad range of temperatures are already tabulated in Dillmann and Meier[23] (for other substances of interest, one may consult the references given therein). With knowledge of macroscopic quatities listed above, the parameters σ_c, τ, and q_0 are evaluated by Eqs. (30), (31), and (32), respectively, where the universal critical exponents β and δ are obtained from Table I (we herein suggest the values $\beta=0.325$, $\delta=4.81\Rightarrow\sigma_c=0.640$ and $\tau=2.208$). The value of σ at any temperature $T\leqslant T_c$ then follows from Eqs. (39) and (40) with C to be taken from Table II (for substances which are

not listed in Table II and for which no experimental data exist, one may, as a first guess, assume a value for C from Table II depending on polarity). For any given temperature T and supersaturation ratio S, the solution of Eq. (36) yields the critical number of molecules i^*. The nucleation rate then follows from Eq. (37).

The above algorithm proposed for calculating nucleation rates by this model has been carried out for a variety of substances in comparison with data available from expansion or diffusion cloud chamber experiments. Figures 2 and 3 show the predictions of the classical nucleation theory [Eq. (38)] and of the new theory [Eqs. (36) and (37)] in an $I–S$ (nucleation rate-supersaturation) plot for water and n-nonane data at various temperatures by Miller[10] and Adams et al.,[14] respectively. The nucleation rates by the classical theory are off by a factor of $10^2–10^3$ for water and by a factor of 10^8 for n-nonane. The new theory yields nucleation rates which are in very good agreement with the experimental data for both water and n-nonane. Figures 4 and 5 show, respectively, the corresponding $S–T$ plots for water against data of Heist and Reiss,[9] Miller,[10] and Anderson et al.[12] and for n-nonane against data of Katz et al.[17,18] and Adams et al.[14] employing both the classical and the new nucleation rate equations. The new nucleation
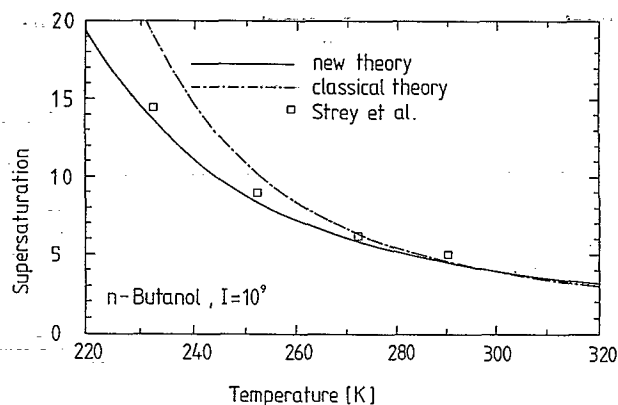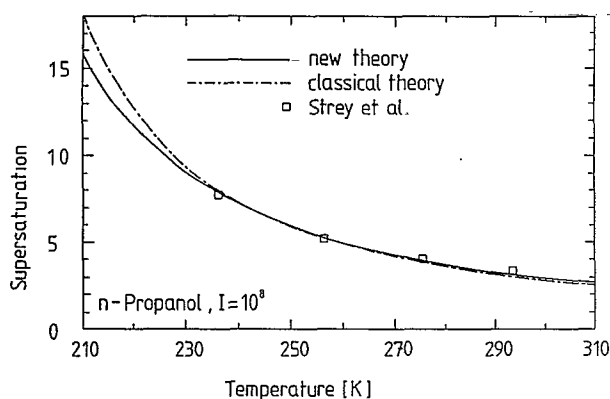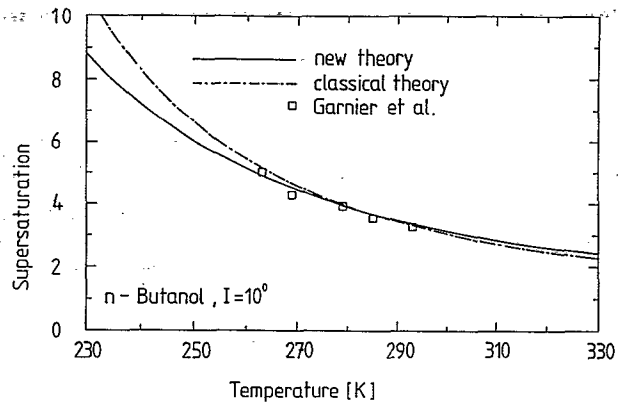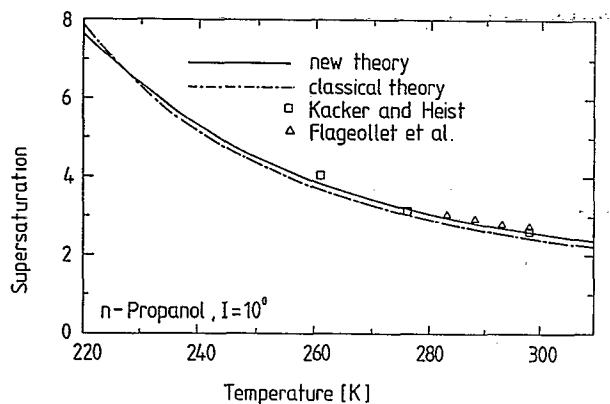
FIG. 8. A comparison of experimental supersaturations with the predictions of the classical theory and the new theory at the constant nucleation rates $I = 10^0$ cm^{-3} s^{-1} and $I = 10^8$ cm^{-3} s^{-1} for n-propanol.

FIG. 9. A comparison of experimental supersaturations with the predictions of the classical theory and the new theory at the constant nucleation rates $I = 10^0$ cm^{-3} s^{-1} and $I = 10^9$ cm^{-3} s^{-1} for n-butanol.

rate equation gives a better agreement with experimental data than the classical one except in comparison with the data by Katz *et al.* for n-nonane which is obviously in disagreement with the data of Adams *et al.* The comparison of the new nucleation rate equation with the classical one against data of Flageollet *et al.*,[11] Garnier *et al.*,[13] and Strey *et al.*[16] for methanol, against data of Kacker and Heist,[15] Garnier *et al.*,[13] and Strey *et al.*[16] for ethanol and n-propanol, and against data of Garnier *et al.*[13] and Strey *et al.*[16] for n-butanol in S-T plots at fixed nucleation rates is illustrated in Figs. 6–9. An overall good agreement with the experimental data over the temperature ranges investigated is achieved by the present nucleation rate equation (37).

VI. CONCLUDING REMARKS

A semiphenomenological droplet model, which corrects for the macroscopic surface tension and monomer–monomer interactions from real gas behavior and generalizes the correlation between the mean surface area of a cluster and the number of molecules contained, is developed as an extension of Fisher's droplet theory of condensation and metastability. A steady-state nucleation rate equation is derived and compared with the classical

Becker–Döring–Zel'dovich nucleation rate equation against the expansion or diffusion cloud chamber data of various vapors. In contrast to the comparison with the classical nucleation rate equation, an overall good agreement with experimental data by the proposed nucleation rate equation is achieved over the range of temperatures investigated ($0.4 \leqslant T/T_c \leqslant 0.6$).

For future investigations, the power law introduced by Eq. (39) for the exponent σ in the expression of the mean surface area can be compared with models from molecular dynamics and further refined yielding more information about the nature of the molecular constant C, which appears as purely empirical in the proposed model. This power law or possibly its refined extension can be checked for substances other than those investigated herein whenever reliable data of nucleation rate for these substances are available.

ACKNOWLEDGMENTS

[1] M. Volmer, *Kinetik der Phasenbildung* (Steinkopff, Dresden, 1939).

[2] A. C. Zettlemoyer, *Nucleation* (Dekker, New York, 1969).

[3] F. F. Abraham, *Nucleation Theory* (Academic, New York, 1974).

[4] M. Volmer and A. Weber, Z. Phys. Chem. **119**, 77 (1926).

[5] L. Farkas, Z. Phys. Chem. **125**, 236 (1927).

[6] R. Becker and W. Döring, Ann. Phys. **24**, 719 (1935).

[7] Y. B. Zel'dovich, Sov. Phys. JETP **12**, 525 (1942).

[8] J. Frenkel, *Kinetic Theory of Liquids* (Oxford University, Oxford, 1946).

[9] R. H. Heist and H. Reiss, J. Chem. Phys. **59**, 665 (1973).

[10] R. C. Miller, Ph.D. thesis, University of Missouri, Rolla, 1976.

[11] C. Flageollet, M. Dinh Cao, and P. Mirabel, J. Chem. Phys. **72**, 544 (1980).

[12] R. J. Anderson, R. C. Miller, J. L. Kassner, Jr., and D. E. Hagen, J. Atmos. Sci. **37**, 2509 (1980).

[13] J. P. Garnier, P. Mirabel, and H. Rabeony, J. Chem. Phys. **79**, 2097 (1983).

[14] G. W. Adams, J. L. Schmitt, and R. A. Zalabsky, J. Chem. Phys. **81**, 5074 (1984).

[15] A. Kacker and R. H. Heist, J. Chem. Phys. **82**, 2734 (1985).

[16] R. Strey, P. E. Wagner, and T. Schmeling, J. Chem. Phys. **84**, 2325 (1986).

[17] J. L. Katz, C. H. Hung, and M. J. Krasnopoler, in *Lecture Notes in Physics*, edited by P. E. Wagner and G. Vali (Springer, New York, 1988), Vol. 309, p. 356.

[18] C. H. Hung, M. J. Krasnopoler, and J. L. Katz, J. Chem. Phys. **82**, 2734 (1985).

[19] J. Lothe and G. M. Pound, J. Chem. Phys. **36**, 2080 (1962).

[20] H. Reiss, J. L. Katz, and E. R. Cohen, J. Chem. Phys. **48**, 5553 (1968).

[21] W. G. Courtney, J. Chem. Phys. **36**, 2009; **36**, 2018 (1962).

[22] J. Feder, K. C. Russell, J. Lothe, and G. M. Pound, Adv. Phys. **15**, 1 (1966).

[23] A. Dillmann and G. E. A. Meier, J. Chem. Phys. **94**, 3872 (1991).

[24] M. E. Fisher, Physics **3**, 255 (1967).

[25] I. J. Ford, J. Aerosol Sci. **23**, 447 (1992).

[26] W. Band, *Quantum Statistics* (Van Nostrand, New York, 1955).

[27] A. H. Wilson, *Thermodynamics and Statistical Mechanics* (Cambridge University, Cambridge, 1966) p. 364.

[28] O. Sinanoğlu, J. Chem. Phys. **75**, 463 (1981).

[29] C. S. Kiang, D. Stauffer, G. H. Walker, O. P. Puri, J. D. Wise, Jr., and E. M. Patterson, J. Atmos. Sci. **28**, 1222 (1971).

[30] R. C. Tolman, J. Chem. Phys. **17**, 333 (1949).

[31] W. Vogelsberger, H. G. Fritsche, and E. Müller, Phys. Status Solidi B **148**, 155 (1988).

[32] D. Stauffer and C. S. Kiang, Phys. Rev. Lett. **27**, 1783 (1971).

[33] D. Beysens, in *Phase Transitions*, edited by M. Lévy, J. C. Guillou, and J. Zinn-Justin (Plenum, New York, 1982), p. 58.

[34] J. E. McDonald, Am. J. Phys. **30**, 870 (1962); **31**, 31 (1963).

[35] B. J. Hiley and M. F. Sykes, J. Chem. Phys. **34**, 1531 (1961).